New Journal of Physics
The open access journal for physics

Diffusion thermopower of a serial double quantum dot

H Thierschmann[1], M Henke[1], J Knorr[1,3], L Maier[1], C Heyn[2], W Hansen[2], H Buhmann[1,4] and L W Molenkamp[1]

[1] Physikalisches Institut (EP3), Universität Würzburg, Am Hubland, D-97074 Würzburg, Germany
[2] Institut für Angewandte Physik und Zentrum für Mikrostrukturforschung, Universität Hamburg, Jungiusstrasse 11, D-20355 Hamburg, Germany
E-mail: hartmut.buhmann@physik.uni-wuerzburg.de

New Journal of Physics **15** (2013) 123010 (8pp)
Received 31 July 2013
Published 6 December 2013
Online at http://www.njp.org/
doi:10.1088/1367-2630/15/12/123010

Abstract. We have experimentally studied the diffusion thermopower of a serial double quantum dot, defined electrostatically in a GaAs/AlGaAs heterostructure. We present the thermopower stability diagram for a temperature difference $\Delta T = (20 \pm 10)\,\mathrm{mK}$ across the device and find a maximum thermovoltage signal of several μV in the vicinity of the triple points. Along a constant energy axis in this regime, the data show a characteristic pattern which is in agreement with Mott's relation and can be well understood within a model of sequential transport.

[3] Present address: Institut für Physikalische und Theoretische Chemie, Universität Würzburg, Am Hubland, D-97074 Würzburg, Germany.
[4] Author to whom any correspondence should be addressed.

Contents

1. Introduction

In recent years the thermopower of one-dimensional and zero-dimensional systems has been investigated widely in experiments and theory [1–5], which led to an increasingly detailed understanding of the energy spectrum and transport properties of systems with reduced dimensionality. It has also been shown that a modification of the electronic density of states is responsible for a strong enhancement of the thermoelectric performance of nano devices and low dimensional structures. In this context, coupled quantum dots (QD) and QD-arrays have been identified as interesting candidates for high performance thermoelectrical devices [6–11], and capable of efficiently converting heat into a directed current on a nanometer scale [12]. However, the overwhelming majority of the work done in this field is of theoretical nature, and, to the authors' knowledge, up to now no thermoelectric characterization of a coupled QD system is available. For single QD structures in the Coulomb blockade regime the thermopower S exhibits a sawtooth-pattern as long as sequential transport is dominant [2, 13]. When cotunneling processes become relevant S is known to be well represented by the Mott-relation [14, 15]—at least as long as correlation effects can be neglected [4]. The Mott relation relates S to the energy derivative of the conductance G at the Fermi level E_f [16] by

$$S_{\mathrm{Mott}} = -\frac{\pi^2}{3}\frac{k^2 T}{e}\frac{1}{G}\left.\frac{\partial G(E)}{\partial E}\right|_{E_f}. \tag{1}$$

Interpreting S in the context of the Kelvin–Onsager-relations $S = \Pi/T$, one can also compare the thermopower with the peltier coefficient $\Pi = I_Q/I$ where I_Q denotes the heat current and I the charge current. This leads to the average energy of charge carriers $\langle E \rangle$ with respect to the Fermi level [17]

$$S = -\lim_{\Delta T \to 0}\frac{V_{\mathrm{th}}}{\Delta T} = -\frac{\langle E \rangle}{eT} \tag{2}$$

with thermovoltage V_{th}, temperature T and the temperature difference ΔT across the system. (2) relates S to the relative energy positions of the transport channels of the nanostructure with respect to the Fermi energy of the reservoirs. Therefore it can be used as a powerful spectroscopy tool for the investigation of the energy levels of a QD system.

In this paper we report on experiments investigating the thermoelectric properties of two coupled QDs in a serial configuration. Measurements of conductance and thermovoltage are presented and it is shown that the thermopower of the double QD (DQD) system is consistent with Mott's relation.

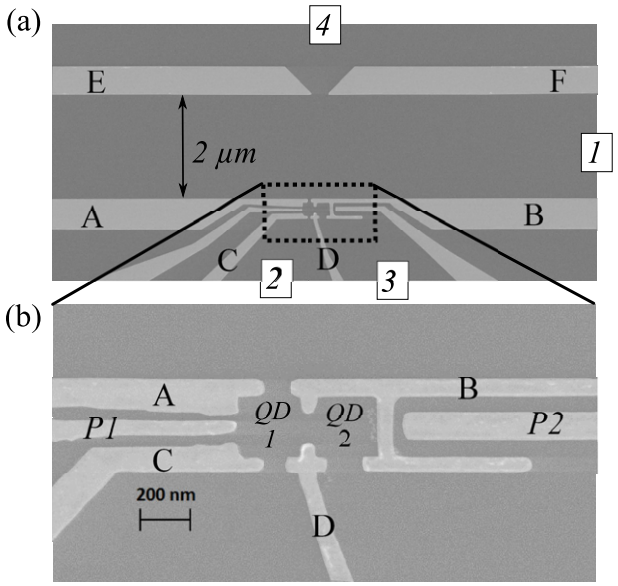

Figure 1. SEM-micrographs of a DQD structure similar to the one used in this work. Regions of dark gray indicate conductive areas, labeled with numbers. The gate electrodes under which the 2DEG can be depleted appear in bright gray and they are denoted with letters A–F, P1 and P2. (a) Larger section of the sample showing the heating channel with QPC and DQD-system on either side. (b) Closeup of the DQD structure.

2. Experiment

The measurements presented here are done on a device fabricated from a GaAs/AlGaAs heterostructure containing a two-dimensional electron gas (2DEG) with a nominal charge carrier density of $n = 2.4 \times 10^{11}\,\mathrm{cm}^{-2}$ and an electron mobility of $\mu = 6.9 \times 10^{5}\,\mathrm{cm}^2\,\mathrm{V}^{-1}\,\mathrm{s}^{-1}$ at 4.2 K. The electron gas is located 92 nm underneath the surface. Ti/Au-electrodes on the surface serve as gates to define the device. Applying a negative voltage to these gates depletes the 2DEG in the region underneath and transfers the gate pattern into the electron gas. Figure 1(a) shows a scanning electron microscopy (SEM) picture of the gate structure. The DQD is formed by gates A, B, C and D. It couples reservoir 1 to the reservoirs 2 and 3. Gates A and B are also part of a heating channel (length: 20 μm, width: 2 μm) defined by gates A, B, E and F. Gates E and F form a quantum point contact (QPC) which is located opposite to the DQD and serves as a reference contact for the thermovoltage measurements. The QPC separating reservoir 4 from the channel, is set to the $10\,e^2\,h^{-1}$ plateau for all experiments.

In figure 1(b) the DQD system is labeled QD1 and QD2, identifying each single QD. The coupling strength of the dots to the reservoirs is controlled by the gate pairs AB, CD and DB, respectively. The DQD-system is adjusted in such a way that the coupling of reservoir 1 to reservoir 2 is very weak ($G_{1,2} \approx 0.001\,e^2/h$). Its contribution to transport remains negligible compared to the coupling of reservoir 1–3 across the DQD which is typically $G_{1,3} \approx 0.3\,e^2/h$. The interdot coupling is controlled by the gates B and D. The plunger gate P1 (P2) is used to change the electrostatic energy of QD1 (QD2). Measurements are performed in a top loader dilution refrigerator at base temperature ($T_{\mathrm{base}} < 70\,\mathrm{mK}$). For characterization measurements

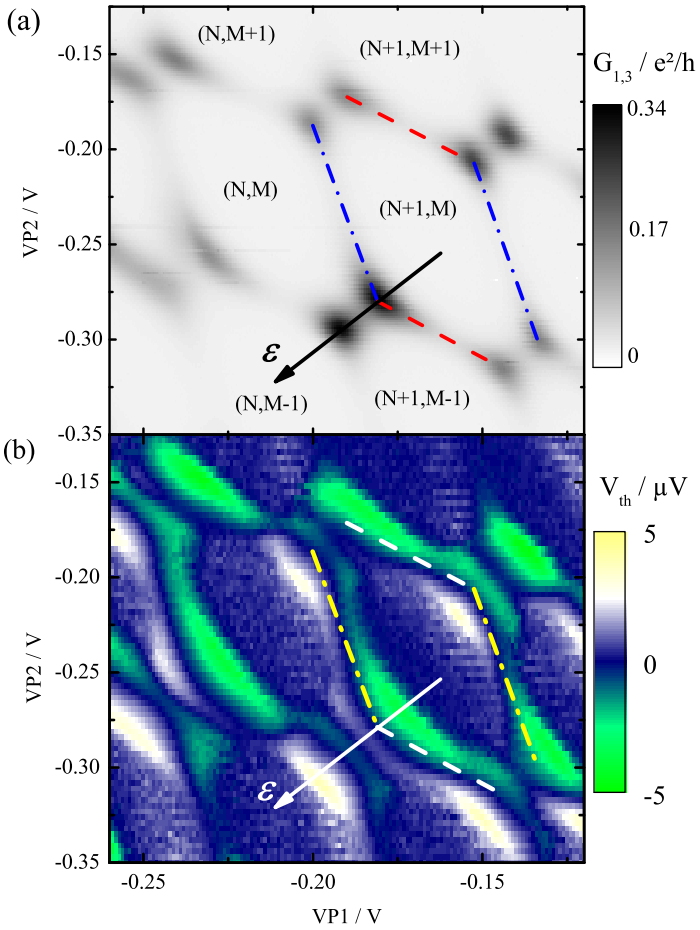

Figure 2. (a) Conductance $G_{1,3}$ and (b) thermovoltage $V_{\rm th}$ stability diagram. The dash-dotted (dashed) lines indicate configurations where only QD1 (QD2) is in resonance with the reservoirs. ε denotes the axis of constant energy of one TP pair along which the QD states stay aligned and are shifted parallel in energy. Thermovoltage data taken for $\Delta T = (20 \pm 10)$ mK.

standard lock-in techniques and a current amplifier are used, with an excitation voltage $U_{\rm ac} = 5\,\mu$V at a frequency $f = 19$ Hz. We estimate that the number of electrons on each dot is of the order of 100, based on the average carrier density in the 2DEG and the lithographic dimensions of the QDs. Figure 2(a) shows the measured stability diagram, displaying the conductance $G_{1,3}$ in a gray scale plot as a function of plunger gate voltages $V_{\rm P1}$ and $V_{\rm P2}$. Dark colors represent high conductance. The stability diagram reveals the usual honeycomb-shaped pattern [19] where each honeycomb originates from a stable charge configuration of the system exhibiting N electrons on QD1 and M electrons on QD2. The lines delimiting each comb correspond to a configuration in which only one dot is in resonance while the other is in a blocking regime. The resonance conditions for QD1 (QD2) are indicated by dashed-dotted (dashed) lines. For weak interdot coupling these lines are expected to be suppressed. The fact that they are slightly visible in the experiment indicates a finite tunnel coupling between the QDs, which enhances cotunneling currents across the device [18]. The corners of each

honeycomb are marked by regions of high conductance, the so-called triple points (TP). Here, the chemical potentials of both dots are aligned with the Fermi energy, E_f, of the reservoirs, which enables sequential transport across the DQD system. The TPs are always split. The splitting is determined by the electrostatic interaction between the dots and by the interdot tunnel coupling energy [19]. From bias dependent measurements the coupling constants α_1 and α_2 are deduced, which relate a change in plunger gate voltage to a change of the individual QD energy. We find $\alpha_1 = 0.0118e$ ($\alpha_2 = 0.0051e$) for the coupling of P1 (P2) and QD1 (QD2). One then obtains charging energies for both dots of about 0.5 meV. From the splitting of two TPs we calculate a total coupling energy E_C of 130–150 μeV. In figure 2(a) the *axis of constant energy*, ε, is indicated by an arrow. Along this axis the charge configurations and relative positions of the energy levels of the QDs remain unchanged while only their position with respect to the chemical potentials of the reservoirs is affected (cf figure 4). Since ε intersects two resonances, the occupation number of the system changes from $(N, M-1)$ to $(N+1, M)$. Between two TPs only one electron is added to the DQD system which is then shared between both dots [19].

For thermopower measurements we use the current heating technique developed previously [1] to establish a defined temperature difference across the DQD: since electron–electron interaction is the dominant scattering mechanism on a length scale of several μm at low temperature, an ac-current ($f = 19$ Hz, $I_{ch} = 22$ nA) passed through the channel leads to a local increase of the electron temperature T_h. Energy dissipation to the lattice takes place in the wide areas of the reservoirs where the electrons thermalize at (lattice) temperature T_c. Hence, a local difference of the electron temperature, $\Delta T = T_h - T_c$, is established between the hot channel and the cooler reservoirs 3 and 4. We estimate a temperature difference ΔT of the order of 20 mK. (To calibrate ΔT we use the QPC as a thermometer, making use of its quantized thermopower $S_{QPC} = S_{QPC}(N, \Delta T)$, where N is the number of conducting modes [1]. For a heating channel with the same geometry made from the same wafer material we find $\Delta T = (20 \pm 10)$ mK for $I_{ch} = 20$ nA at base temperature.) Due to the fact that the dissipated heating power is proportional to the square of the current in the channel, $P \propto I_{ch}^2$, ΔT oscillates with a frequency $2f$. Using a lock-in amplifier at $2f$ we detect the generated thermovoltage signal between reservoir 4 and 3, $V_{th} = V_{th,\,DQD} - V_{th,\,QPC}$. Since the QPC is now set to a conductance plateau, its contribution to the measured signal is negligible [1] and the detected voltage is directly related to the thermovoltage generated by the DQD-system.

Figure 2(b) shows the thermovoltage data V_{th} in a color scale plot for the same stability parameters as the conductance characterization. It can be seen that the thermovoltage stability diagram retraces the honeycomb pattern of the conductance. Remarkably, features which only give rise to a weak conductance signal, e.g. the lines delimiting the honeycombs, show a strong thermovoltage signal. In those areas V_{th} exhibits distinct positive and negative contributions which resemble the thermopower signal of a single QD [14].

Even more interesting is the pronounced structure of positive and negative thermovoltage around each pair of TPs and in particular in between two adjacent TPs. For further analysis we plot the thermovoltage data along the ε-axis for all six TP pairs which are shown in figure 2(b). In a first order approximation α_1 and α_2 can be used to convert the voltage axis into the appropriate energy scale, $\varepsilon = \sqrt{(\alpha_1 \Delta V_{P1})^2 + (\alpha_2 \Delta V_{P2})^2}$. The result is given in figure 3(a): the thermovoltage shows a characteristic line shape which is similar for all TP pairs.

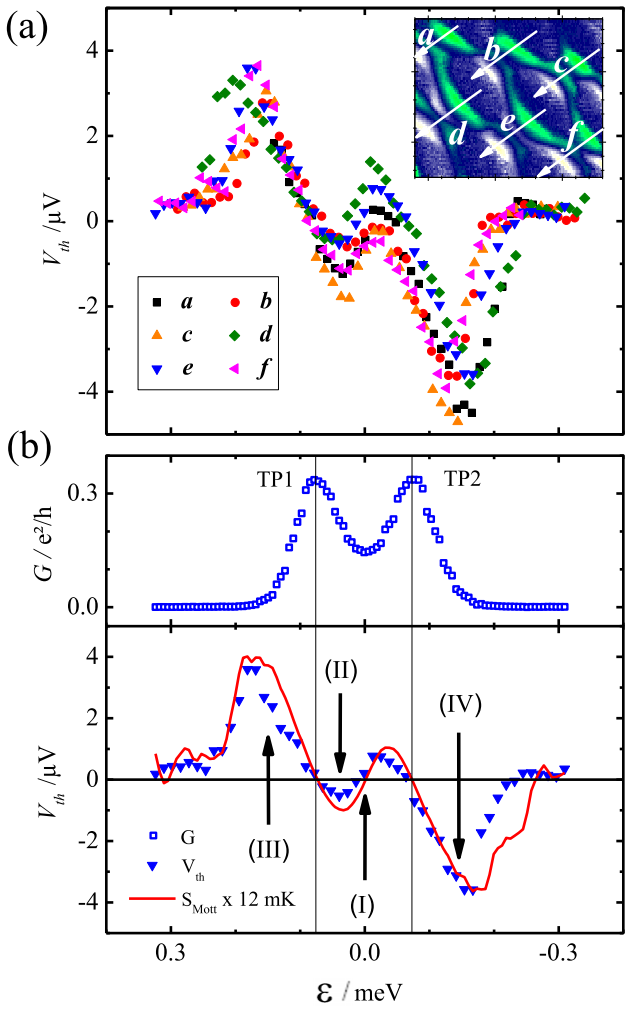

Figure 3. (a) V_{th} extracted for all TP pairs from the thermovoltage stability diagram along the respective ε-axis. $\varepsilon = 0$ was chosen to be at the center of the TP pair. (b) Conductance G (top, blue squares) and thermovoltage V_{th} (bottom, blue triangles) data for TP pair ***e***. Red line: Mott-thermovoltage calculated from the conductance data and (1) using $T = 230$ and $\Delta T = 12$ mK.

3. Discussion

As an example, figure 3(b) compares the thermovoltage and conductance data along the ε axis for TP ***e*** (see inset of figure 3(a)). $\varepsilon = 0$ is defined at the center between the two TP conductance peaks ((I) in figure 3(b)). Note that epsilon increases with decreasing gate voltages as indicated by the arrows in figure 2 and the inset in figure 3. For increasing ε, the thermovoltage first decreases, reaching a minimum at $\varepsilon = 0.05$ meV (II) and then becomes positive at $\varepsilon = 0.07$ meV. It increases (III) until it reaches a maximum of +4.0 μV and then decays until it becomes zero again for $\varepsilon > 0.25$ meV. For negative ε we observe the same behavior but with an inverted sign (IV). The sign changes occur at the maxima of G and at $\varepsilon = 0$.

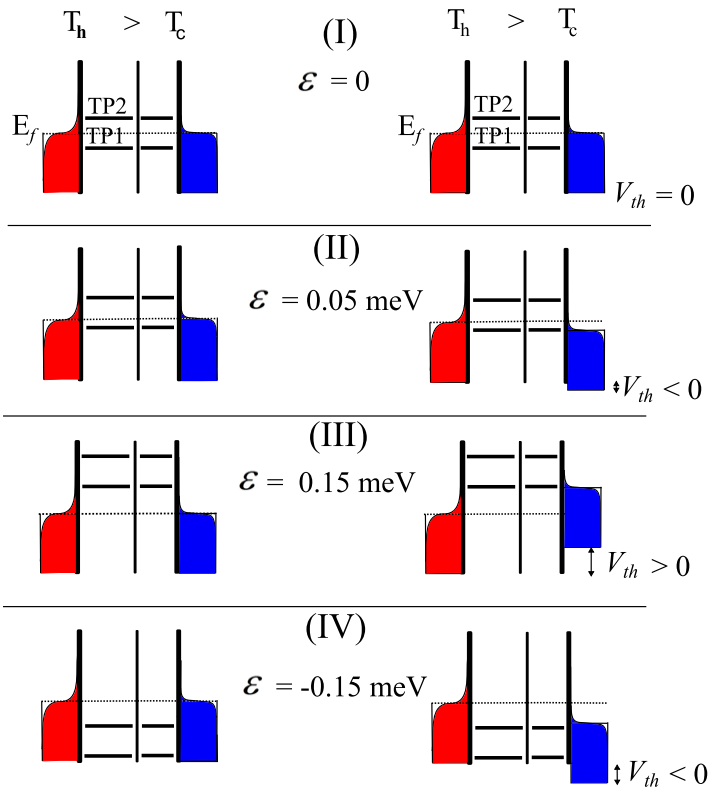

Figure 4. Energetic positions of the DQD resonances TP1 and TP2 for different ε as indicated in figure 3(b). Left column without, right column with built up thermovoltage.

The variation of V_{th} can be explained as follows: from (2) we understand that V_{th} is related to the average energy of the charge carriers contributing to transport with respect to the Fermi level. At $\varepsilon = 0$ the system is in a symmetric state, i.e. the two TPs TP1 and TP2 are energetically located symmetrically around the Fermi level of the reservoirs (cf figure 4(I)). Consequently, any temperature driven current across the DQD cancels out. These currents consist of electrons moving from the hot to the cold reservoir involving energy level TP2 and energy level TP1 for electrons transferred in the opposite direction. The average energy of the charge carriers equals the chemical potentials in the reservoirs and therefore the system remains in its initial state with a resulting $V_{\mathrm{th}} = 0$. Rising or lowering ε breaks this symmetry. For small $\varepsilon > 0$, TP1 approaches the Fermi level, while TP2 is moved further away. This leads to an enhanced charge transfer across TP1 while reducing currents via TP2. Hence, a net electron drain from the cold reservoir to the hot causes the chemical potential of the cold reservoir to decrease until a current equilibrium is re-established (figure 4(II)) which gives rise to a negative thermovoltage signal. A further increase of the electrostatic energy of the system, $\varepsilon > 0.07$ meV, shifts both TPs above the Fermi level (figure 4(III)). In this regime only hot carriers contribute to the charge transfer, which raises the chemical potential of the cold reservoir and leads to a high thermovoltage signal. For $\varepsilon > 0.18$ meV the transmission probability of hot carriers decreases and the thermovoltage signal approaches zero. For $\varepsilon < 0$ the mechanisms are the same with inverted symmetry, i.e. that for example in the case of $\varepsilon = -0.15$ meV (figure 4(IV)) transport

is only possible for electrons from the cold reservoir until the equilibrium is reached resulting in a negative thermovoltage signal.

The observed line shape resembles the derivative of G indicated by the Mott-relation (1). To verify this assumption we calculate the Mott-thermopower from the smoothed conductance data. The result is shown in figure 3(b) (red line). Clearly, the Mott result indeed reproduces the line shape of V_{th}. For $\Delta T = 12$ and $T = 230\,\mathrm{mK}$ (estimated from the conductance resonance line shape) we obtain a good quantitative agreement with the experimental data. Finally, we note that previous theoretical treatments predicted additional features in the thermopower signal between two TPs due to the formation of symmetric and antisymmetric molecular states [7, 9, 11]. We suggest that the fact, that we do not observe these features in our experiments results from the relatively high electron temperature in our system.

In conclusion, we have presented thermovoltage data of a DQD structure. We have used the current heating technique at dilution refrigerator temperatures to obtain a temperature difference $\Delta T = (20 \pm 10)\,\mathrm{mK}$. The DQD system has been investigated in a serial configuration yielding the thermopower stability diagram. A maximum thermovoltage of several μV is observed in the vicinity of the TP pairs. Along the axis of constant energy, the thermovoltage shows a characteristic curve which is consistent with Mott's relation and can be well understood in a simple DQD picture of sequential transport.

Acknowledgments

This work has been financially supported by the DFG (SPP 1386).

References

[1] Molenkamp L W, van Houten H, Beenakker C W J, Eppenga R and Foxon C T 1990 *Phys. Rev. Lett.* **65** 1052
[2] Staring A A M, Molenkamp L W, Alphenaar van Houten H, Buyk O J A, Mabesoone M A A, Beenakker C W J and Foxon C T 1993 *Europhys. Lett.* **22** 57
[3] Godijn S F, Möller S, Buhmann H, Molenkamp L W and van Langen S A 1999 *Phys. Rev. Lett.* **82** 2927
[4] Scheibner R, Buhmann H, Reuter D, Kiselev M N and Molenkamp L W 1995 *Phys. Rev. Lett.* **95** 176602
[5] Eltschka C and Siewert J 2011 arXiv:1111.2629v1
[6] Cai J and Mahan G 2008 *Phys. Rev.* B **78** 035115
[7] Chen X, Buhmann H and Molenkamp L W 2000 *Phys. Rev.* B **61** 16801
[8] Humphrey T and Linke H 2005 *Phys. Rev. Lett.* **94** 096601
[9] Wierzbicki M and Swirkovicz R 2010 *J. Phys.: Condens. Matter* **22** 185302
[10] Rajput G and Sharma K C 2011 *J. Appl. Phys.* **110** 113723
[11] Chi F, Zheng J, Lu X-D and Zhang K-C 2011 *Phys. Lett.* A **375** 1352
[12] Sánchez R and Büttiker M 2011 *Phys. Rev.* B **83** 085428
[13] Beenakker C W J and Staring 1992 *Phys. Rev.* B **86** 9667
[14] Scheibner R, Novik E G, Borzenko T, König M, Reuter D, Wieck A D, Buhmann H and Molenkamp L W 2007 *Phys. Rev.* B **75** 041301
[15] Andreev A V and Matveev K A 2001 *Phys. Rev. Lett.* **86** 280
[16] Cutler M and Mott N F 1969 *Phys. Rev.* **181** 1336
[17] Matveev K A and Andreev A V 2002 *Phys. Rev.* B **66** 045301
[18] Gustavsson S, Studer M, Leturcq R, Ihn T and Ensslin K 2008 *Phys. Rev.* B **78** 155309
[19] van der Wiel W G, De Franceschi S, Elzerman J M, Fujisawa T, Tarucha S and Kouwenhoven L P 2002 *Rev. Mod. Phys.* **75** 1